24th INTERNATIONAL CONGRESS ON SOUND AND VIBRATION
23–27 July 2017, London

NUMERICAL MODELLING OF THE GROUND-BORNE VIBRATIONS GENERATED BY TRUCK-ROAD INTERACTION

Georges Kouroussis, Loïc Ducarne and Daniel Ainalis
University of Mons, Faculty of Engineering, Department of Theoretical Mechanics, Dynamics and Vibrations, Mons, Belgium
email: georges.kouroussis@umons.ac.be

Like railway-induced ground vibrations, ground-borne motions generated by the passing of heavy vehicles in urban areas are one of the fundamental problems in transport annoyance in the vicinity of buildings. In presence of local geometries like a speed bump or pavement defects, wheels interact with the road surface and cause dynamic motions in the vehicle that reacts with the road and generates high level vibrations that propagate in the soil through complex waves and impinge on the foundations of nearby structures. The scope of this study is twofold. The first part is dedicated to the prediction of vibration levels using a two-step approach. A multibody approach is used for the vehicle modelling, including the tyre/bump/road interaction. A finite element analysis is used for the next approach, calculating the ground wave propagation of a moving load, defined as the output of the first calculation. A decoupled simulation is possible due to the large stiffness of the road compared to the stiffness characteristics of the vehicle (tyre). A validation is performed using experimental data available in the literature. The second part focuses on a sensitivity analysis in order to identify the main parameters (bump geometry, speed, ...) that affect the shape and level of peak particle velocity at various distances from the road. In light of the study, the prediction scheme offers an efficient way to design speed bumps and to understand the complex waves generated by a transient moving load propagating in an infinite medium.

Keywords: tyre/road interaction, ground waves, finite element analysis, speed bump, multibody simulation

1. Introduction

Although the development of alternative means of transport to road networks have emerged in recent decades, the road freight transport remains important in Europe, with several huge flows in countries such as Poland, Germany and France. The flexibility in terms of selected travel and of goods travelled is the reason of this successful transport activity, although there are more opportunities to substitute road transport with more environmentally friendly modes. In addition to pollution issues, road transport generates ground-borne vibration and noise that have a significant influence on the quality of the life and the vibration and acoustic environment [1]. Surely, due to the limited weight per axle and the limited speed compared to a railroad network, freight vehicles, including buses, trucks and other heavy vehicles, generally induce less vibration levels [2–4] but, when the road surface is not smooth, comparable ground-borne vibrations can be observed [5].

Practically, the road-induced ground vibrations are produced by the varying forces between tyre and road when the vehicle passes over important singular defects in the road. The effect becomes perceptible in neighbouring buildings in the frequency range 8–16 Hz [6]. Hildebrand et al. [7] demonstrated that, for a sufficiently soft and compactable soil, the vehicle and soil responses are not independent and coupling is necessary in such specific situations. In other cases, if the road has a large stiffness compared to the vehicle's tyre or suspension stiffness, the entire configuration can be uncoupled and the vehicle and the road/ground can be considered as two separate problems [8]. This modelling approach offers a complete framework to evaluate the dynamics of a moving vehicle and the tyre/road interaction [9], along with the ground wave propagation in a close distance from the singular defect, including the free field [10] and the built environment [11, 12]. For this second case, transfer function analysis, boundary element methods or finite element methods are often retained to compute the expected results.

The aim of this paper is the development of a prediction model composed of well-suited modelling approaches for each subsystem. A validation is then performed using free trials available in [13] and a sensitivity analysis is presented to study the influence of the geometry and shape of speed bumps.

2. Calculating the tyre/road forces using the multibody approach

A typical 3D model of a vehicle moving on an asphalt road is displayed in Fig. 1. The position and orientation of each body (car body, wheelsets and other inertial components, systems or elements) are gathered into the configuration parameters q_i. The positions of the suspension are also presented.

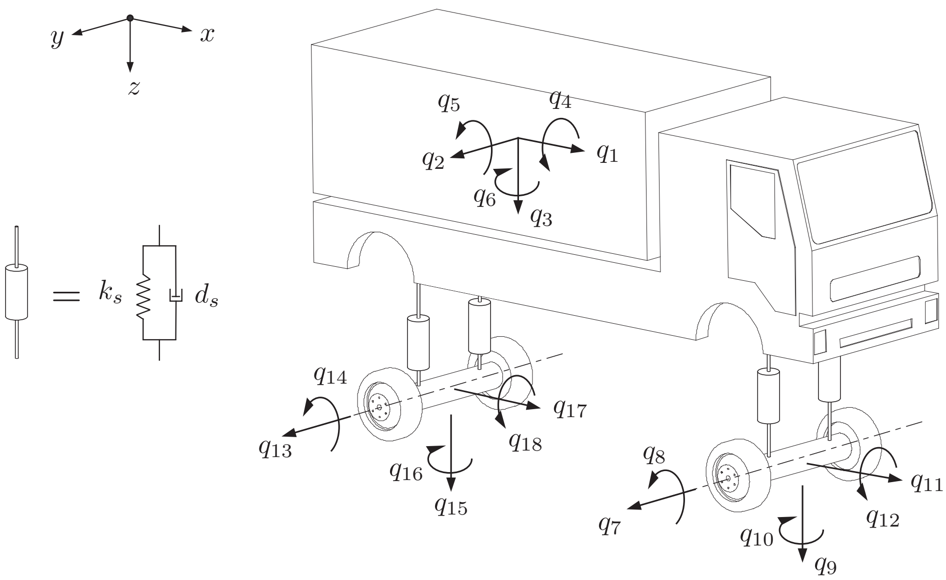

Figure 1: Vehicle multibody model (exploded view), including the selection of configuration parameters and modelling of the suspension system.

The approach with minimal coordinates [14] is used to build a system of ordinary differential equations for the vehicle. The configuration parameters are chosen, in a number n_{cp} corresponding to the number of degrees of freedom (denoted by q_j). This approach has the advantage to automatically eliminate all the joint forces and allows for efficient integration with existing numerical techniques. If the system is comprised of n_B bodies, only n_{cp} equations can be built around the n_{cp} configuration parameters. The application of d'Alembert's principle leads to the following equations of motion

$$\sum_{i=1}^{n_B} \left[\underline{\mathbf{d}}^{i,j} \cdot (\underline{\mathbf{R}}_i - m_i \underline{\mathbf{a}}_i) + \underline{\theta}^{i,j} \cdot (\underline{\mathbf{M}}_{Gi} - \Phi_{G_i} \dot{\underline{\omega}}_i - \underline{\omega}_i \times \Phi_{G_i} \underline{\omega}_i) \right] = 0 \;\; j = 1, \ldots, n_{cp} \tag{1}$$

with m_i and Φ_{G_i} the mass and the central inertia tensor of body i, $\underline{\mathbf{R}}_i$ and $\underline{\mathbf{M}}_{Gi}$ the resultant force and moment, at the centre of gravity G_i, of all applied forces exerted on body i, $\underline{\mathbf{a}}_i$ the acceleration of the centre of gravity of body i, $\underline{\mathbf{d}}^{i,j}$ the partial contributions of $\dot{q}_j$ in the velocity $\underline{\mathbf{v}}_i$ of the centre of gravity of body i and $\underline{\theta}^{i,j}$ the partial contributions of $\dot{q}_j$ in the rotational velocity $\underline{\omega}_i$ of body i

$$\underline{\mathbf{v}}_i = \sum_{j=1}^{n_{cp}} \underline{\mathbf{d}}^{i,j} \cdot \dot{q}_j \tag{2}$$

$$\underline{\omega}_i = \sum_{j=1}^{n_{cp}} \underline{\theta}^{i,j} \cdot \dot{q}_j \ . \tag{3}$$

Eq. (1) can become tedious to elaborate due to the difficulty in defining the complex motion of some bodies and due to many successive derivation (velocities and accelerations in both translational and rotational directions).

The homogeneous transformation matrix approach, which gives the situation of the associated local frame with respect to another frame as a function of the configuration parameters, offers an elegant way to define the bodies' motion. For any complex mechanical system, the motion of each body can be decomposed into a succession of elementary motions (rotation about one axis, pure translational displacement) defined as successive multiplications of simple matrices. This 4×4 matrix has the general well–known form

$$\mathbf{T}_{i,j} = \begin{pmatrix} \mathbf{R}_{i,j} & \{\underline{\mathbf{r}}_{j/i}\}_i \\ 0\,0\,0 & 1 \end{pmatrix} \tag{4}$$

where $\underline{\mathbf{r}}_{j/i}$ is the coordinate vector of frame j with respect to frame i, and $\mathbf{R}_{i,j}$ is the rotation tensor describing the orientation of frame j with respect to frame i. To obtain the kinematics ($\underline{\mathbf{v}}_i$, $\underline{\mathbf{a}}_i$, $\underline{\omega}_i$, $\underline{\dot{\omega}}_i$) and the partial contributions ($\underline{\mathbf{d}}^{i,j}$, $\underline{\theta}^{i,j}$), only differentiation operations on terms of homogeneous transformation matrices are necessary.

The proposed approach was implemented in an object-oriented C++ program, using the in-house EasyDyn library [15]. The kinematics and the partial contributions of Eq. (1) are obtained using the symbolic tool CaGeM. It also creates a C++ code directly compilable against the EasyDyn library which is completed by the applied forces (suspensions) and the link with the ground. The EasyDyn library was written in C++ and provides 4 modules:

- the vec module, introducing classes related to vector calculus: vectors, rotation tensors, inertia tensors, and homogeneous transformation matrices;
- the sim module to integrate second-order differential equations;
- the mbs module, a front-end to sim module which automatically builds the differential equations of motion of a multibody system from the kinematics and the applied forces;
- the visu module, allowing to build scenes composed of moving objects and directly usable with the associated animation tool EasyAnim.

Its purpose is to help users to set up and integrate the equations of motion of a multibody system with minimal effort. These several modules allow:

- the generation of bodies kinematics from the position information using the symbolic tool called CaGeM,
- the numerical building of equations of motion, using the bodies kinematics and the definition of the forces applied on the mechanical system,
- the integration of these equations written in residual form,
- the animation of the scenes, for a better visualization of the motion.

A detailed description of the framework can be found in [15, 16]. The EasyDyn framework has been successfully applied on train/track dynamic problems [17, 18] and more recently on vehicle/bridge interaction problems [19].

In order to understand how the vehicle interacts with the road and the speed bump, a tyre model was implemented in EasyDyn. The tyre element is considered as a force relationship based on Fromm's model [20]. The distribution of vertical pressure in the contact zone is parabolic along the circumference so that a tyre could be compared to an assembly of springs in the longitudinal, radial and lateral directions as shown in Fig. 2.

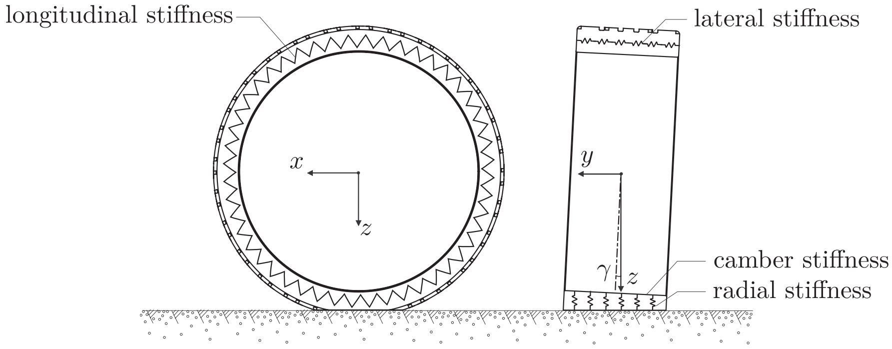

Figure 2: Tyre equivalent spring modelling.

3. Ground vibration assessment using finite element modelling

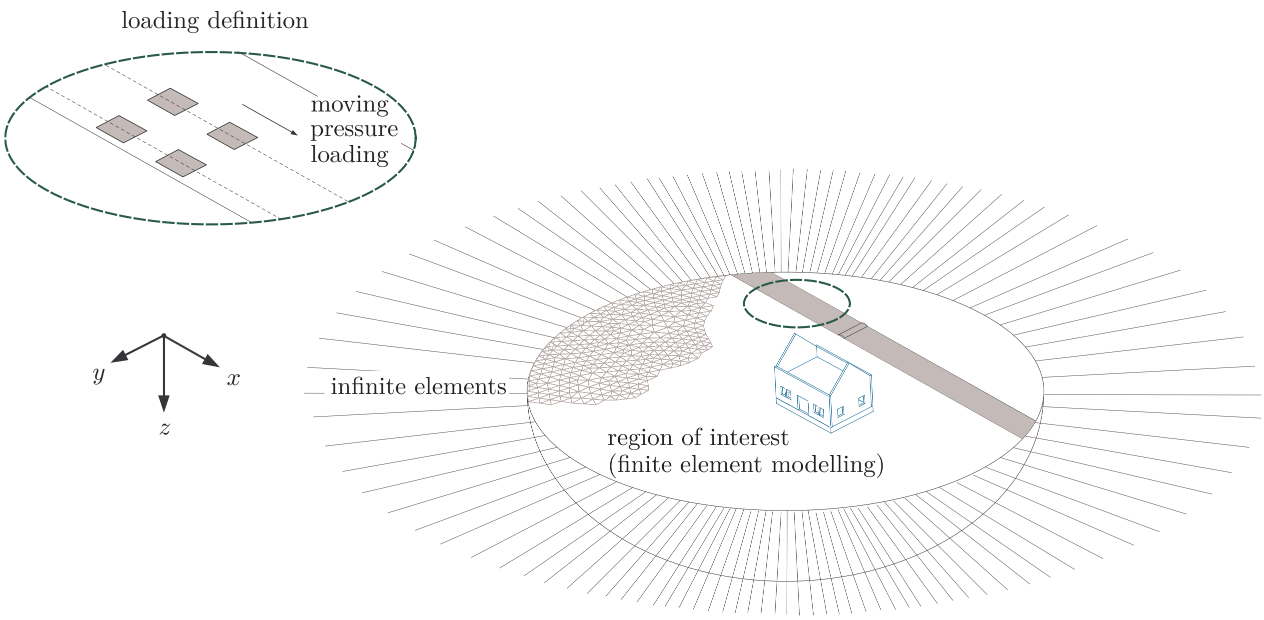

Figure 3: Ground modelling.

The second step is concerned with the soil, whose free field response is computed from the loads acting on the soil surface (using finite element analysis), issued from the first subproblem (Fig. 3). The simulation is performed in the time domain using an implicit scheme. The use of infinite elements, coupled with appropriate viscous boundary conditions [21, 22], mimics the effect of infinity. Practically, the soil simulation is performed using the ABAQUS software package (the choice of ABAQUS as a simulation platform was motivated by the presence of infinite elements within its library, on the contrary to other soil mechanics software packages). It has been shown that time response analysis is more appropriate to simulate vibration wave propagation: as a transient dynamic problem, it is naturally represented in the time domain. The proposed approach offers the possibility to consider three-dimensional models, with the usual computer resources. Additionally, linear and non-linear behaviour can be easily implemented, as well as complex geometry (embankment, inclined layer interfaces, variability in road profile, ...). This ranks the finite element method on the same level as the boundary element method [23]. Particular attention was paid to the following:

- *Proper boundary conditions*. The combined use of viscous boundaries and infinite elements provides a more efficient non-reflecting condition than classical setups (free or fixed boundaries). Here, the small dependence on incident wave angle and dynamic parameters is quantitatively carried out for each solution. A spherical soil border geometry is defined, to which infinite elements are attached and with a viscous boundary at the interface of finite/infinite elements in order to better absorb implying waves. As the domain size does not affect the boundary efficiency, reasonable domain size can be considered with low computation time.
- *Accurate loading description*. In order to represent the contact forces between the tyres and the road, the best method was to create a moving pressure load. To achieve this, a pressure was applied on surfaces that represent the contact area between the tyre and the road. This contact surface must then move along another surface that represents the tyre path as shown on Fig. 3. The simulation of a moving pressure on ABAQUS requires the use of a custom user subroutine written in Fortran defining the non-constant value of the pressures.

4. Validation

The validation was performed using experiments available in [13]. The vehicle model is based on the Volvo FL6 truck. Due to the physical conditions and the limited information about the vehicle parameters, only the motion of the vehicle in the vertical plane was retained. An Irons-Guyan reduction was applied by Lombaert [24] to verify the effectiveness of the reduced number of degrees of freedom for the present application. The geometrical and inertial data are provided in [24]. The number n_{cp} of configuration parameters q_j is fixed to 7 (according to Fig. 1, degrees-of-freedom q_2, q_4, q_6, q_7, q_{10}, q_{12}, q_{13}, q_{16}, q_{18} are locked to 0), according to the selected pitch and bounce motions of each body. From the general vehicle dimensions and the vehicle speed $v_0 = \dot{q_1}$ (constant), the homogeneous transformation matrices $\mathbf{T}_{0,i}$ of each body i is expressed with the help of elementary motions as a displacement $\mathbf{T}^{\text{disp}}(x, y, z)$ or a rotation $\mathbf{T}^{\text{rot. } y}(\theta)$ about the y-axis. Translational and rotational velocities and accelerations are derived from the symbolic tool and the external forces (suspensions, gravity and tyre/road contact) are defined, in order to numerically obtain the equations of motion, as described by Eq. (1).

Figures 4 and 5 compare the results predicted by the proposed model with experimental data provided in [24]. A trapezoidal traffic plateau (height $h = 54\,\mathrm{mm}$ and total length $l = 1.7\,\mathrm{m}$) was used as a speed bump during the experiments and the same geometry was implemented for the simulations. The vehicle speed was a constant $30\,\mathrm{km/h}$. A good correlation is observed between both results with some discrepancies: the predicted time histories overestimate the maximum level, especially for the rear axle load impact on the artificial unevenness. The frequency content is relatively well reproduced within the frequency range 0–50 Hz, with however a small difference: the predicted magnitude is greater in the frequency range 0–20 Hz, but slightly lower within 20–50 Hz. At this stage of comparison and with some unknown parameter values (e.g. tyre characteristics), the model can be considered as validated.

5. Sensitivity analysis

Figure 6 shows the effect of speed bump geometry and vehicle speed on the vibration level in terms of PPV. Regarding the speed bump, two geometries were investigated: the reference bump with a trapezoidal plateau and a different smooth shape modelled by a half-sine. For the vehicle's speed, two speeds — $30\,\mathrm{km/h}$ and $60\,\mathrm{km/h}$ — were considered. The peak particle velocity

$$PPV = \max(\text{abs}(v_z(t))) \tag{5}$$

was used as main indicator and computed from the velocity time history $v_z(t)$ in the vertical direction. The influence of the defect geometry is clearly visible in Fig. 6(a) where a strong difference is ob-

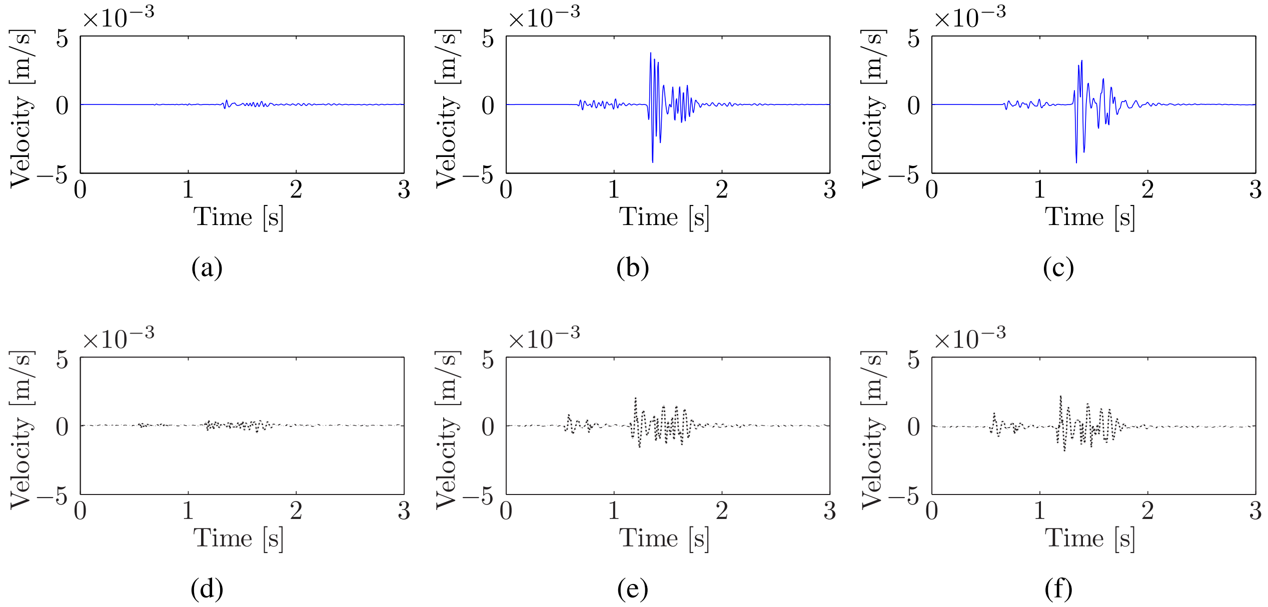

Figure 4: Predicted (top) and measured (bottom) vibration velocities at $8\,\mathrm{m}$ from the road, for a Volvo FL6 truck travelling at $30\,\mathrm{km/h}$ on a speed bump of height $h = 54\,\mathrm{mm}$ and length $l = 1.7\,\mathrm{m}$: x-component (left), y-component (middle), z-component (right).

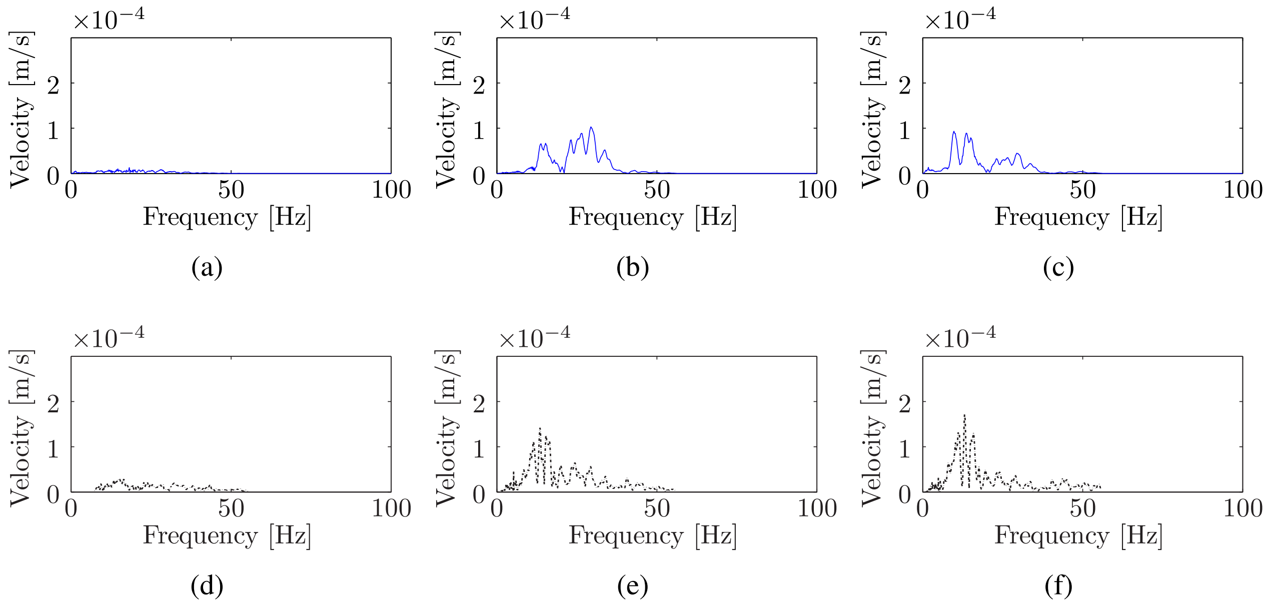

Figure 5: Predicted (top) and measured (bottom) vibration frequency spectra at $8\,\mathrm{m}$ from the road, for a Volvo FL6 truck travelling at $30\,\mathrm{km/h}$ on a speed bump of height $h = 54\,\mathrm{mm}$ and length $l = 1.7\,\mathrm{m}$: x-component (left), y-component (middle), z-component (right).

served between the trapezoidal and half-sine geometries, although they have a relatively similar size. Figure 6(b) shows the effect of vehicle speed, with a vibration level twice as high than in the reference case. This latter observation corroborates with the well-known fact that speed bumps generally have a negative vibration effect for high-speeds, when the vehicle runs over the speed limitations that impose such speed control.

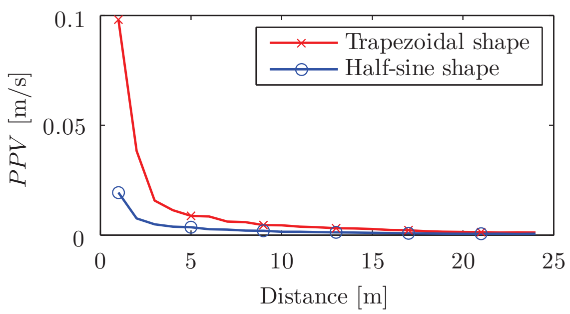

(a)

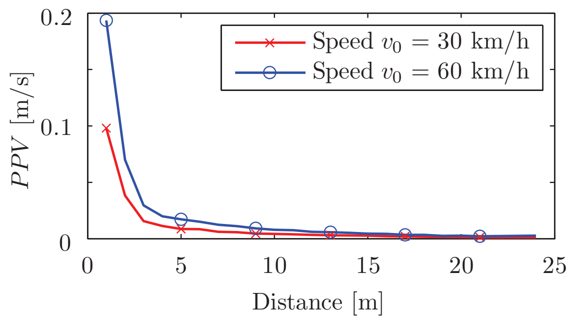

(b)

Figure 6: Predicted PPV as a function of distance from the road: (a) effect of the speed bump shape; (b) effect of the vehicle speed.

6. Conclusion

Heavy truck-induced ground vibrations can cause negative effects on local communities situated near the road networks. These vibrations are a consequence of the vehicle forces acting from the wheels onto singular unevenness. This paper showed a prediction model combining finite element analysis and multibody approach. Several aspects were emphasized and the results obtained proved that the proposed approach offers a useful tool to assess vibration control problems related to road traffic.

REFERENCES

1. Vogiatzis, K. and Kouroussis, G. Environmental road transportation noise monitoring: a necessary tool for the protection & rehabilitation of the urban acoustic environment, *Proceedings of the 24th International Congress on Sound and Vibration*, London (UK), (2017).

2. Lu, Z., Hu, Z., Yao, H. and Liu, J. Field evaluation and analysis of road subgrade dynamic responses under heavy duty vehicle, *International Journal of Pavement Engineering*, **(in press)**, (2016).

3. Connolly, D. P., Kouroussis, G., Laghrouche, O., Ho, C. and Forde, M. C. Benchmarking railway vibrations — track, vehicle, ground and building effects, *Construction and Building Materials*, **92**, 64–81, (2015).

4. Connolly, D. P., Marecki, G., Kouroussis, G., Thalassinakis, I. and Woodward, P. K. The growth of railway ground vibration problems — a review, *Science of the Total Environment*, **568**, 1276–1282, (2016).

5. Lak, M., Degrande, G. and Lombaert, G. The effect of road unevenness on the dynamic vehicle response and ground-borne vibrations due to road traffic, *Soil Dynamics and Earthquake Engineering*, **31** (10), 1357–1377, (2011).

6. Watts, G. and Krylov, V. Ground-borne vibration generated by vehicles crossing road humps and speed control cushions, *Applied Acoustics*, **59** (3), 221–236, (2000).

7. Hildebrand, R., Keskinen, E. and Navarrete, J. A. R. Vehicle vibrating on a soft compacting soil half-space: Ground vibrations, terrain damage, and vehicle vibrations, *Journal of Terramechanics*, **45** (4), 121–136, (2008).

8. Lombaert, G., Degrande, G. and Clouteau, D. Numerical modelling of free field traffic-induced vibrations, *Soil Dynamics and Earthquake Engineering*, **19** (7), 473–488, (2000).

9. Pyl, L., Degrande, G., Lombaert, G. and Haegeman, W. Validation of a source-receiver model for road traffic induced vibrations in buildings. I: Source model, *ASCE Journal of Engineering Mechanics*, **130** (12), 1377–1393, (2004).

10. Lombaert, G. and Degrande, G. Experimental validation of a numerical prediction model for free field traffic induced vibrations by in situ experiments, *Soil Dynamics and Earthquake Engineering*, **21** (6), 485–497, (2001).

11. Pyl, L., Degrande, G. and Clouteau, D. Validation of a source-receiver model for road traffic induced vibrations in buildings. II: Receiver model, *ASCE Journal of Engineering Mechanics*, **130** (12), 1394–1406, (2004).

12. Zhang, Y., Zhang, N., Cao, Y. and Xia, H. A prediction method of historical timber buildings vibrations induced by traffic loads and its validation, *Shock and Vibration*, **Vol. 2017** (article ID 1451483), 12 pages, (2017).

13. Lombaert, G., Degrande, G. and Clouteau, D. The influence of the soil stratification on free field traffic-induced vibrations, *Archive of Applied Mechanics*, **71** (10), 661–678, (2001).

14. Hiller, M. Dynamics of multibody system with minimal coordinates, Pereira, M. and Ambrosio, J. (Eds.), *Computer-Aided Analysis of Rigid and Flexible Mechanical Systems, Proceedings of the NATO Advanced Study Institute*, Tróia, (Portugal), pp. 119–163, (1993).

15. Verlinden, O., Ben Fekih, L. and Kouroussis, G. Symbolic generation of the kinematics of multibody systems in EasyDyn: from MuPAD to Xcas/Giac, *Theoretical & Applied Mechanics Letters*, **3** (1), 013012, (2013).

16. Kouroussis, G., Rustin, C., Bombled, Q. and Verlinden, O. EasyDyn: multibody open–source framework for advanced research purposes, J. C. Samin, P. F. (Ed.), *Multibody Dynamics 2011*, Brussels (Belgium), ECCOMAS Thematic Conference, (2011).

17. Kouroussis, G., Van Parys, L., Conti, C. and Verlinden, O. Prediction of ground vibrations induced by urban railway traffic: an analysis of the coupling assumptions between vehicle, track, soil, and buildings, *International Journal of Acoustics and Vibration*, **18** (4), 163–172, (2013).

18. Kouroussis, G., Connolly, D. P., Vogiatzis, K. and Verlinden, O. Modelling the environmental effects of railway vibrations from different types of rolling stock — a numerical study, *Shock and Vibration*, **Vol. 2015** (article ID 142807), 16 pages, (2015).

19. Daniel, L., Olivier, B., Kortis, J. and Kouroussis, G. Modelling of road vehicle–bridge interaction using a compound multibody/finite element approach, *Proceedings of the 23rd International Congress on Sound and Vibration*, Athens (Greece), (2016).

20. Gim, G., *Vehicle dynamic simulation with a comprehensive model for pneumatic tires*, Ph.D. thesis, University of Arizona, (1988).

21. Lysmer, J. and Kuhlemeyer, R. L. Finite dynamic model for infinite media, *Journal of the Engineering Mechanics Division, Proceedings of the ASCE*, **95** (EM4), 859–877, (1969).

22. Kouroussis, G., Verlinden, O. and Conti, C. Finite-dynamic model for infinite media: corrected solution of viscous boundary efficiency, *ASCE Journal of Engineering Mechanics*, **137** (7), 509–511, (2011).

23. Kouroussis, G., Van Parys, L., Conti, C. and Verlinden, O. Using three-dimensional finite element analysis in time domain to model railway–induced ground vibrations, *Advances in Engineering Software*, **70**, 63–76, (2014).

24. Lombaert, G., *Development and experimental validation of a numerical model for the free field vibrations induced by road traffic*, Ph.D. thesis, Katholieke Universiteit te Leuven, (2001).